New HVDC Transmission System Using Three-Phase Two-Level Converters

Rui Filipe Batista Rum Castro, Instituto Superior Técnico

Abstract

As technology evolves, the need and possibility to transmit electrical energy across long distances, using aerial transmission lines or sub aquatic cables, steadily increased. For long distances it can be more advantageous that the transmission happens in direct current (DC) instead of the classical alternate current (AC), as its losses are reduced and no problems related to reactive power exist.

In this work is presented a transmission system that allows energy flow at high power and voltage levels by use of a multi-level architecture involving multiple two-level converters, rated for lower voltages and powers than the the ones used by the system. By using multiple two-level converters in series it is possible to achieve multi-level operation as opposing to two-level operation. In order to achieve such results, this power system makes use of open-end winding transformers, filters and also controllers, such as current, power and voltage controllers, in order to establish the transferred power and the voltage level at which the power transfer occurs.

The designed system was developed and tested in Matlab, being subject to various tests and operating conditions. At the end of this work, the obtained results are analyzed, highlighting the relevancy of the passive filters and it comes to conclusion that, in general, the high efficiency of the system, the multi-level operation and the relatively low total harmonic distortion (THD) of the relevant waveforms turn this work in a viable proposal.

1. Introduction

1.1. Motivation

The use of HVDC (High Voltage Direct Current) systems is mainly related to some advantages compared to the transmission system of electrical energy in sinusoidal alternating form at high voltage (HVAC, *High Voltage Alternating Current*).

Firstly, sinusoidal AC transmission systems present some difficulties when it comes to connecting multiple networks because of the need for synchronisation between them. The direct current transmission system overcomes this difficulty because, for each network, alternating currents (AC) are converted into direct current (DC), allowing, regardless of the operating frequency of each network, the connection between them to be made without having to take into account the frequency of each network [1; 2]. This positive point contributes to an increase in the stability of each network by allowing the transfer of energy between networks that, previously, would have been incompatible. In addition, the fact that energy is transferred in direct current also contributes to simplifying the existence of power transmission control, since there is no active power transfer and, unlike sinusoidal alternating transmission systems, the transmission of energy over long distances does not require reactive compensation [1; 2].

Another important advantage to mention of the HVDC transmission system compared to the alternating current transmission system is related to the corona effect on the conductors and the distance at which the transfer can be made. DC transmission has lower corona effect losses compared to sinusoidal AC transmission, which makes radio interference lower compared to AC transmission system [3; 4] and through the use of DC transmission it is possible to have underwater power transfer, for example, to cross sea arms and or to make connections of offshore wind farms and also air power transfer over medium and long distances.

Initially, HVDC transmission systems were based on Current Source Converters (CSC) consisting of Line Commuted Converters (LCC). Although this technology is effective in the transfer of energy at very high voltages, it does not provide reactive power control in the AC interconnection and also presents significant harmonic distortion.

With the technological development and the availability of controlled and more robust semiconductor devices, such as GTO (Gate Turn-off Thyristor) and IGBT (Insulated Gate Bipolar Transistor), have contributed to the use of VSC (Voltage Source Converters) within the HVDC power transfer. This topology of using VSC allows operation at switching frequencies much higher than the grid frequency and, in comparison with LCC technology, allows reactive power control and a decrease of filters to mitigate harmonic distortion in the conversion process.

This method of power transfer, in direct current, has been standing out over time as an alternative to the most common methodology for power transmission - AC current based systems. The high voltages at stake (1 MV) require the use of hundreds of power semiconductor devices associated in series. Given the difficulty in simultaneously

switching all the semiconductors in the series, multilevel converter structures have imposed themselves on HVDC VSC. However, many multilevel converters are complex in terms of capacitors, isolated voltage sources, voltage balance, so there is an attempt to use common converter associations, called two-level

The motivation for this dissertation is the fact that the implementation of a multilevel system based on bi-level converters allows reducing the negative aspects of a multilevel HVDC system using multilevel converters. The two-level converters are known and relatively simple converters, compared with other topologies, leading, for example, to a lower complexity in what concerns to the control system, although for high voltages they still require series associations of power semiconductors. In Figure 1 is presented a classic HVDC transmission system topology.

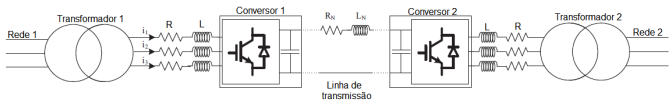

Figure 1: Schematic of a simple HVDC transmission system, adapted from [2].

1.2. Objectives

The main objectives of this MSc dissertation include the topology definition, modelling, simulation and control of a new multilevel HVDC transmission system, using four two-level three-phase converters (and respective transformers) as the interface with the electrical grid, so that sinusoidal alternating current power is converted into direct current and can thus be transmitted in DC. For this, the most common types of converters for HVDC will be briefly analysed. Special focus will be given to the two-level converter.

The piecemeal objectives are:

- Define the new topology;
- Dynamically model the new topology;
- Simulate in open loop the new topology;
- Design (synthesize) controllers for the HVDC power transmission system;
- Test the dynamic performance of the new system.

1.3. Document structure

This document is divided into six parts. The first part is the introduction, where the motivation, objectives and general structure of this document are presented. The second part contains the converter structure and connections, as well as some fundamental equations. Part three describes the functioning of the system and its topology. Part four is where the controllers that allow the system to operate are developed. In the fifth part the results obtained from simulating the proposed system in different situations are analysed and the sixth part contains the conclusions drawn from the analysis of the obtained results, as well as possible future work in order to improve the proposed topology.

2. Converter analysis and connections

In Figure 2 it is shown how it would be possible to make the connection of the two-level full-bridge converter to the two terminals of an open-end windings transformer. Essentially, each winding will have a voltage in phase opposition (relative to the voltage of the first terminal) connected to the second terminal of the winding that is usually used to connect the transformer to the earth electrode.

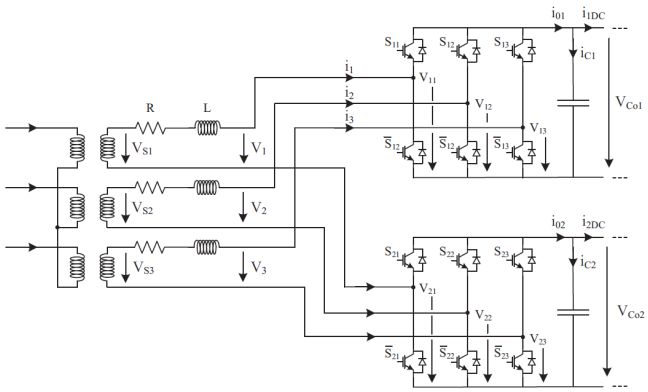

Figure 2: Schematic of the connection of two three-phase two-level converters to the secondary of an open-winding transformer, adapted from [2].

The phase voltages are given by the equations in (1), considering that $V_1 = V_{11} - V_{21}$.

$$\begin{aligned} V_1 &= \frac{2V_{11} - V_{12} - V_{13}}{3} - \frac{2V_{21} - V_{22} - V_{23}}{3} \\ V_2 &= \frac{2V_{12} - V_{13} - V_{11}}{3} - \frac{2V_{22} - V_{23} - V_{21}}{3} \\ V_3 &= \frac{2V_{13} - V_{11} - V_{12}}{3} - \frac{2V_{23} - V_{21} - V_{22}}{3} \end{aligned} \tag{1}$$

Which can be written in its matrix form:

$$\begin{bmatrix} V_1 \\ V_2 \\ V_3 \end{bmatrix} = \begin{bmatrix} \frac{2}{3} & -\frac{1}{3} & -\frac{1}{3} \\ -\frac{1}{3} & \frac{2}{3} & -\frac{1}{3} \\ -\frac{1}{3} & -\frac{1}{3} & \frac{2}{3} \end{bmatrix} \cdot \begin{bmatrix} V_{11} \\ V_{12} \\ V_{13} \end{bmatrix} - \begin{bmatrix} \frac{2}{3} & -\frac{1}{3} & -\frac{1}{3} \\ -\frac{1}{3} & \frac{2}{3} & -\frac{1}{3} \\ -\frac{1}{3} & -\frac{1}{3} & \frac{2}{3} \end{bmatrix} \cdot \begin{bmatrix} V_{21} \\ V_{22} \\ V_{23} \end{bmatrix} \tag{2}$$

This topology grants multi-level operation in the AC voltages, as shown in Figure 3.

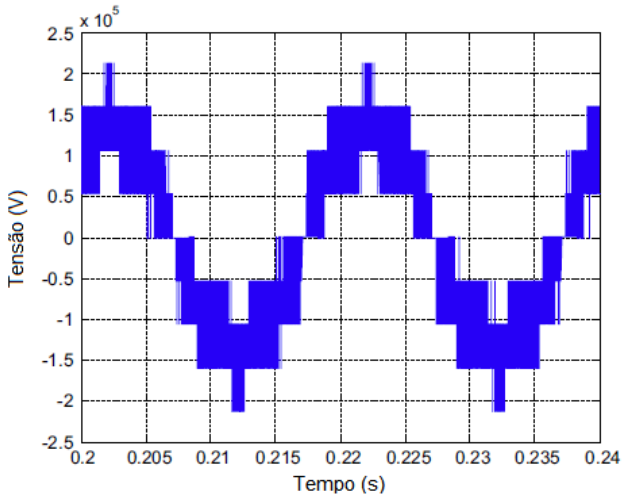

Figure 3: AC output voltage for the proposed system, adapted from [2]

3. System topology

An HVDC transmission system contains both emitter-side and receiver-side converters. Additionally, the transmission is usually bi-directional, i.e., power can flow from the emission to the reception and vice versa. In this dissertation, only two transformers are considered at the emission and two transformers at the reception, so there will be eight two-level three-phase full-bridge converters - four converters at the sending side and four converters at the receiving side - with each pair of converters in series. Figure 4 shows the topology proposed for this four-cable transmission system.

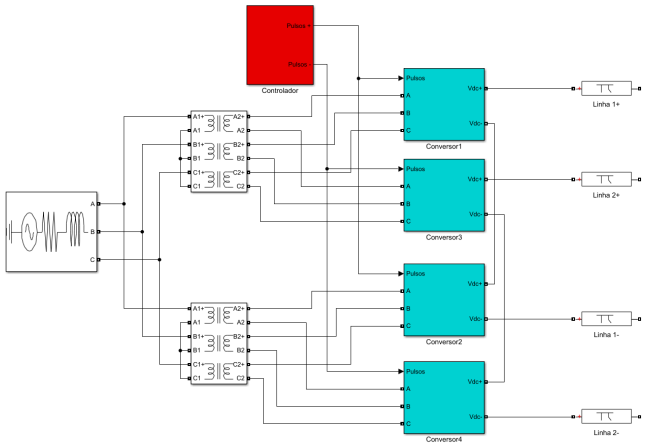

Figure 4: Four-wire multi-port HVDC transmission system using four three-phase two-level converters.

These converters are connected to the electrical grid (represented by non-ideal voltage sources) by means of a transformer which, at each secondary terminal (each phase), is connected to an inductive filter. On the DC side of each converter, there is a capacitor whose function is to filter the voltage seen by the transmission line. The transmission lines are represented by the π model [5] of each of the four cables, considering the resistance, inductance and capacitance between each cable and ground. At last, a RLC series filter is added on the AC voltages side as a solution to reduce the harmonic distortion (THD) of the transmission system, as shown in Figure 5 [6].

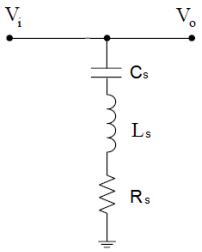

Figure 5: RLC series filter.

In the case under study in this dissertation it is considered 500 MW as the maximum transmitted power, and this value can be varied, according to the needs of the networks, through the implemented controllers. The DC voltage level considered is $U_{dc_T} = 490\,\text{kV}$ and, considering that there are two pairs of converters in series, each converter presents half of the total transmission voltage to its terminals, that is, $U_{dc} = 245\,\text{kV}$, value that corresponds to the working voltage of the selected transmission cable.

4. Control Design

Each converter is controlled by a controller on each side of the transmission system. One side of the system controls the voltage at which the transmission occurs, while the opposite side controls the power transmitted by the system. These controllers operate on the AC side currents by use of pulse width modulation (PWM).

Figure 6 shows each converter's variables and directions considered in order to design the control system for the converters.

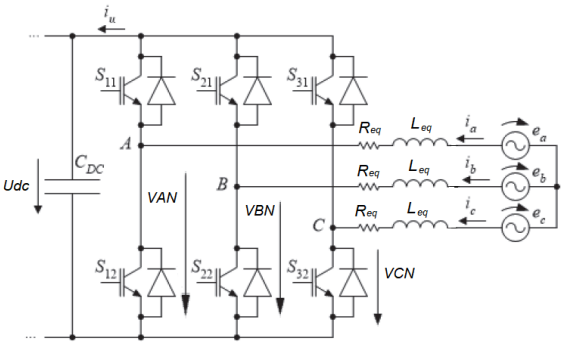

Figure 6: Converter variables - current and voltage directions considered.

4.1. AC Current Control

The equations for each phase of the converter's three-phase system are shown in (3).

$$\begin{cases} \dfrac{di_a}{dt} = -\dfrac{V_{AN}}{L_{eq}} - \dfrac{R_{eq}}{L_{eq}} \cdot i_a + \dfrac{e_a}{L_{eq}} \\ \dfrac{di_b}{dt} = -\dfrac{V_{BN}}{L_{eq}} - \dfrac{R_{eq}}{L_{eq}} \cdot i_b + \dfrac{e_b}{L_{eq}} \\ \dfrac{di_c}{dt} = -\dfrac{V_{CN}}{L_{eq}} - \dfrac{R_{eq}}{L_{eq}} \cdot i_c + \dfrac{e_c}{L_{eq}} \end{cases} \tag{3}$$

By applying Clark and Park's Transform the equations in a bi-dimensional reference are obtained:

$$\begin{cases} \dfrac{di_d}{dt} = -\dfrac{u_d}{L_{eq}} - \dfrac{R_{eq}}{L_{eq}} \cdot i_d + \omega i_q + \dfrac{e_d}{L_{eq}} \\ \dfrac{di_q}{dt} = -\dfrac{u_q}{L_{eq}} - \dfrac{R_{eq}}{L_{eq}} \cdot i_q - \omega i_d + \dfrac{e_q}{L_{eq}} \end{cases} \tag{4}$$

The equations show cross-terms in each component. However, by considering $H_{id} = -u_d + L_{eq}\omega i_q + e_d$ and $H_{iq} = -u_q - L_{eq}\omega i_d + e_q$ the system becomes linearised, as shown in equations (5).

$$\begin{cases} \dfrac{di_d}{dt} = -\dfrac{R_{eq}}{L_{eq}} \cdot i_d + \dfrac{H_{id}}{L_{eq}} \\ \dfrac{di_q}{dt} = -\dfrac{R_{eq}}{L_{eq}} \cdot i_q + \dfrac{H_{iq}}{L_{eq}} \end{cases} \tag{5}$$

The developed current controller's schematic is presented in Figure 7.

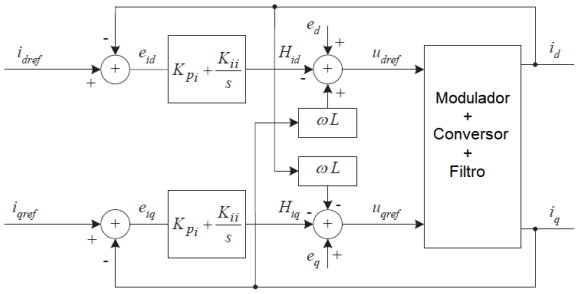

Figure 7: Schematic of the developed current controller.

4.2. Power Control

With the current controller developed, it is possible to elaborate an active and reactive power controller based on alternating currents.

The instantaneous three-phase active and reactive power in $dq0$ coordinates are given by equations (6).

$$\begin{cases} P = e_d \cdot i_d + e_q \cdot i_q \\ Q = -e_d \cdot i_q + e_q \cdot i_d \end{cases} \tag{6}$$

Considering that the d of the rotating referential, originated due to park's transform, is aligned with phase a of the electrical grid $v_q = 0$ and the equations simplify. Therefore, by choosing active and reactive power references (P_{ref} and Q_{ref}), current references $i_{d_{ref}}$ and $i_{q_{ref}}$ are generated in the current controller.

$$\begin{cases} i_{d_{ref}} = \dfrac{P_{ref}}{e_d} \\ i_{q_{ref}} = -\dfrac{Q_{ref}}{e_d} \end{cases} \tag{7}$$

The developed schematic is presented in Figure 8.

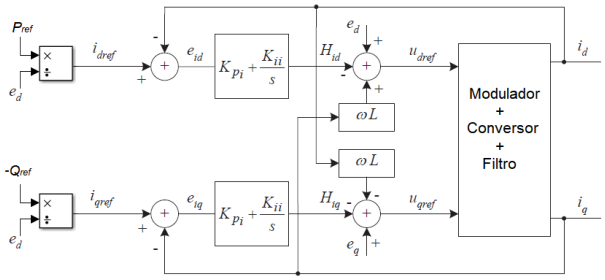

Figure 8: Schematic of the developed three-phase active and reactive power controller.

4.3. DC Voltage Control

Considering the connection on the DC side of the two-level converter, shown in Figure 9, it is possible to write the DC voltage's equation, written in (8).

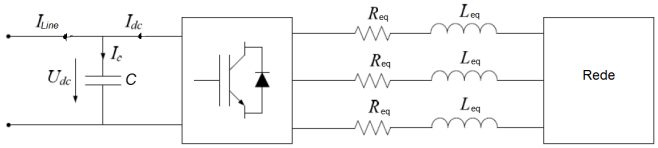

Figure 9: Simplified two-level converter connection diagram.

$$\frac{dU_{dc}}{dt} = \frac{1}{C}\left(\frac{e_d}{U_{dc}} \cdot i_d - I_{line}\right) \tag{8}$$

The developed control diagram is shown in Figure 10.

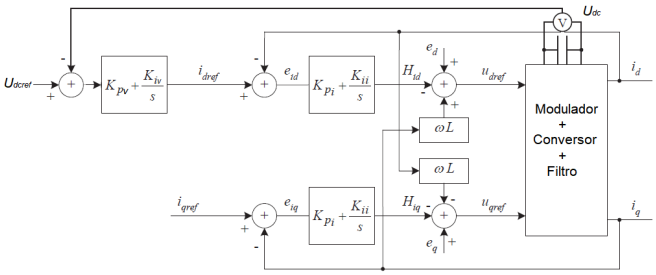

Figure 10: Schematic of the developed voltage controller.

5. Simulation Results

5.1. Rated Power Operation

In Figure 11 and Figure 12 are the waveforms of the phase to ground three-phase voltages on the emitter side of the system and the currents of the system.

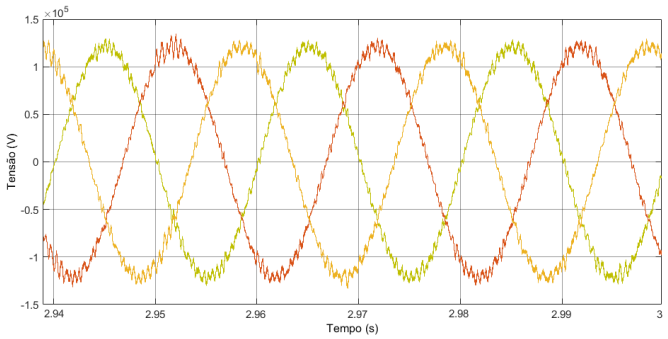

Figure 11: Three-phase voltages on the receiver side of the transmission system.

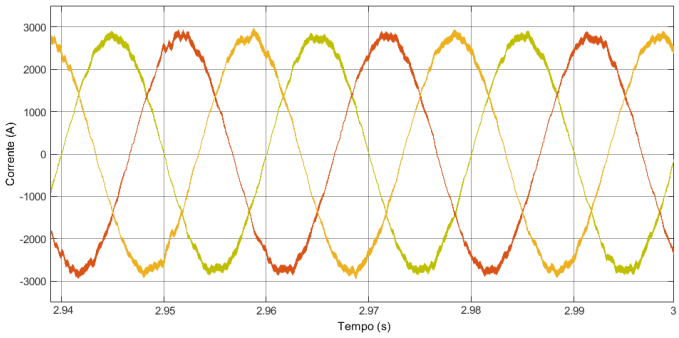

Figure 12: Three-phase currents on the receiver side of the transmission system.

As can be observed, due to the non-idealities of the developed system, despite the existence of the developed series RLC filter, the three-phase voltages present some harmonic distortion (as well as the currents). However, the filters cannot be dismissed since the harmonic distortion, in comparison with the results obtained from the system without the series RLC filters, is very low.

In Figures 13 and 14 the three-phase quantities of the sender system in the absence of series RLC filter are represented. Note that in this situation, due to the distortion of the three-phase voltages their measured amplitude appears to be higher, which in turn affects the three-phase currents, because the power controller uses these voltages to act and control the transmitted power in the system by controlling the currents, also increasing the amplitude of the currents.

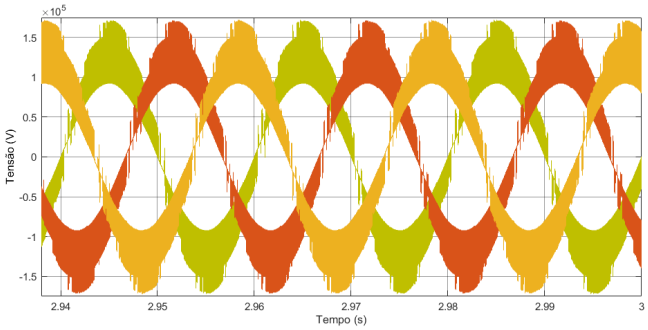

Figure 13: Three-phase voltages on the receiver side of the transfer system in the absence of RLC filter.

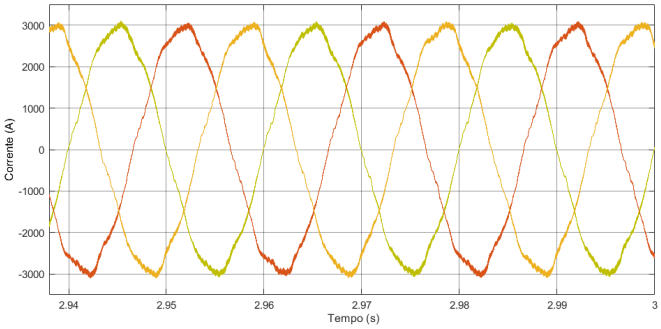

Figure 14: Three-phase currents on the receiver side of the transfer system in the absence of RLC filter.

For a more precise analysis, the harmonic spectrum of the three-phase voltages and currents was analysed in both situations (with filter and without filter) and the results were compared. In the following figures there are the spectral analyses of the mentioned values.

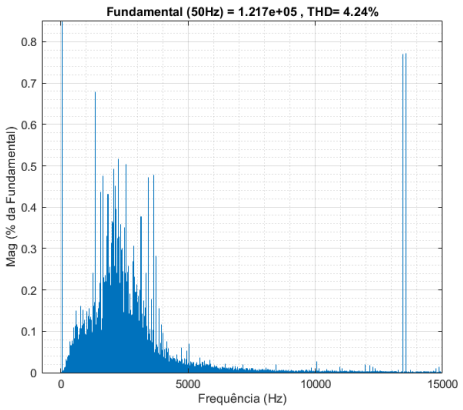

Figure 15: Spectral analysis of three-phase voltages with series RLC filter.

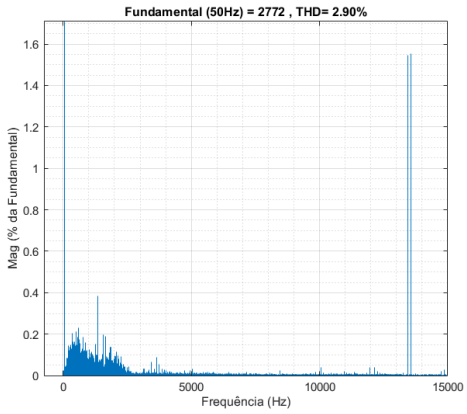

Figure 16: Spectral analysis of three-phase currents with series RLC filter.

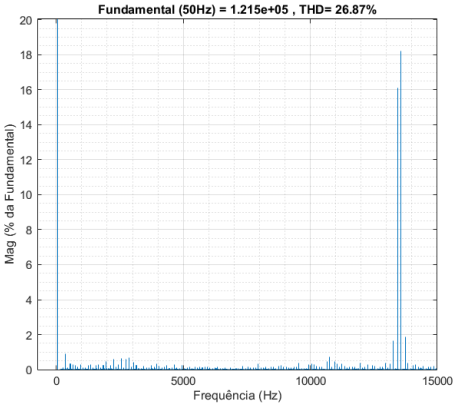

Figure 17: Spectral analysis of three-phase voltages without filter.

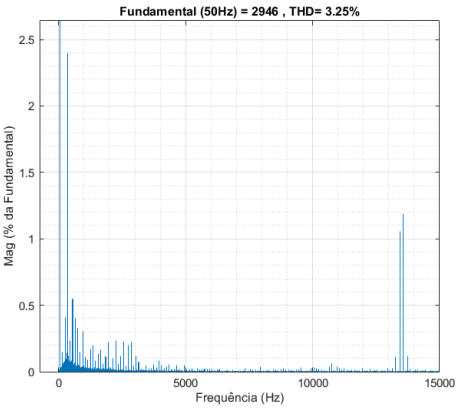

Figure 18: Spectral analysis of three-phase currents without filter.

Table 1 contains the THD values for a simpler analysis.

Total Harmonic Distortion (THD)	With RLC Filter	Without RLC Filter
Voltage	4.24%	26.87%
Current	2.90%	3.25%

Table 1: Comparative table of the harmonic distortion values of the three-phase quantities.

Figures 19 and 20 show the currents controlled by the power controller and the voltage controller, respectively.

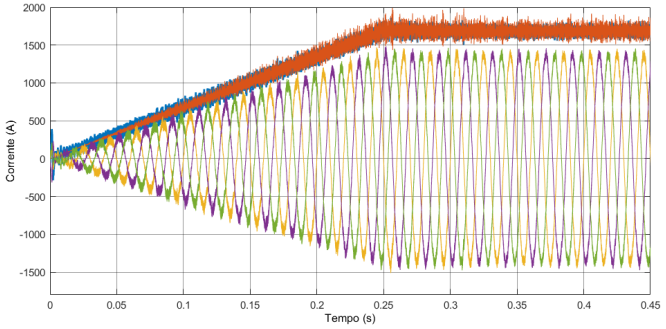

(a) Controlled currents following reference signal (in orange).

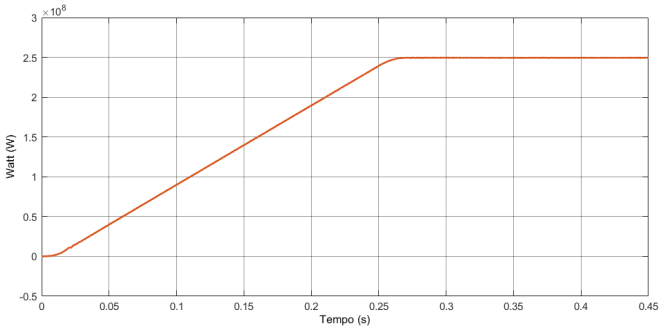

(b) Initial transient of the controlled power.

Figure 19: Power controller in operation.

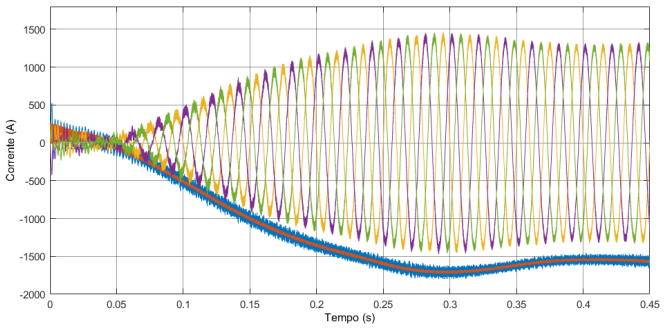

(a) Controlled currents following reference signal (in orange).

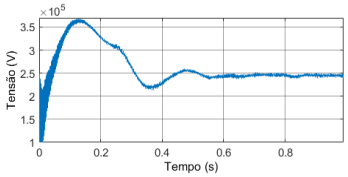

(b) Initial transient of the controlled voltage U_{dc}.

Figure 20: Voltage controller in operation.

As can be seen, the voltage controller, unlike the power controller, has a negative reference signal, because the positive reference on the receiver side means that it consumes power, so the current flows from the emitter side to the receiver side, i.e. the current on the system side where the voltage is controlled is negative. Thus, observing the three-phase components of the emitter side, it is natural that the current and voltage are out of phase 180° as it corresponds to the power being emitted, as shown in Figures 21 and 22.

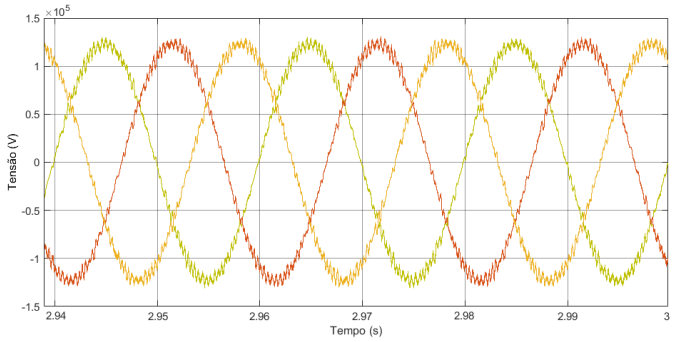

Figure 21: Three-phase voltages on the emitter side of the transmission system.

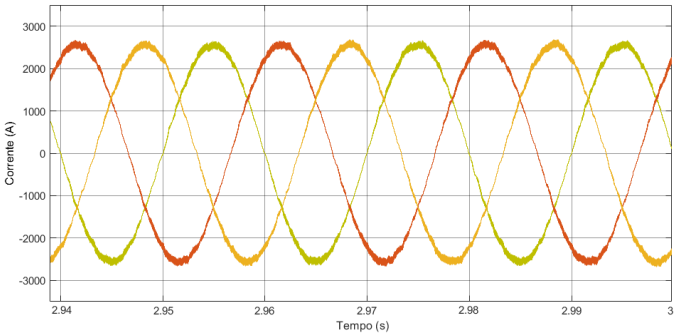

Figure 22: Three-phase currents on the emitter side of the transmission system.

As for the DC quantities, Figures 23 and 24 show the transmission line voltages and currents, respectively.

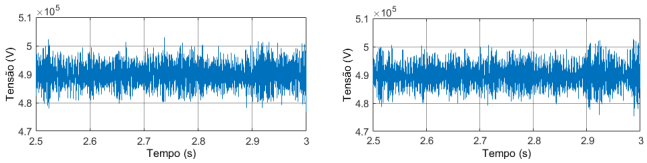

(a) Transmission voltage between converters 1 and 2.

(b) Transmission voltage between converters 3 and 4.

Figure 23: Transmission voltage between each pair of transmission lines.

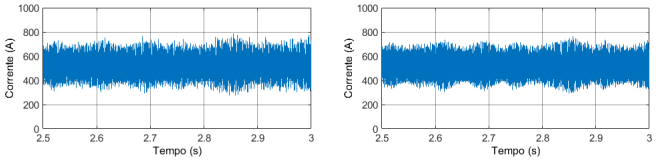

(a) DC current flowing through converters 1 and 2.

(b) DC current flowing through converters 3 and 4.

Figure 24: Transmission current flowing through positive transmission lines.

In Figure 25 one can observe the transmitted and received power at the secondary terminals of each transformer, which turns out to be half of the transmitted power, i.e. 250 MW, which corresponds to the reference power of the power controller.

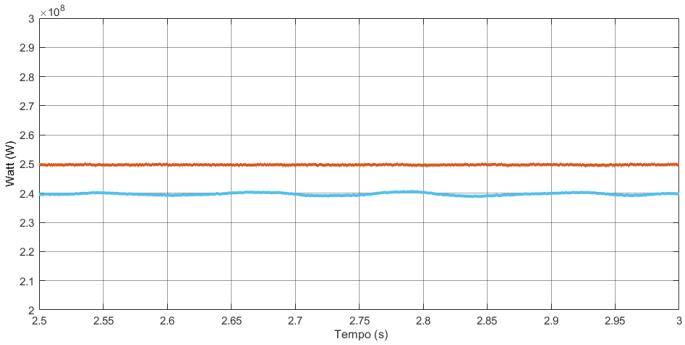

Figure 25: Transmitted/received (orange graph) and received (blue graph) power by each converter pair (in half the system).

Using this measurement in Figure 25, it can be seen that the system efficiency (including losses in the transmission lines, filter coils and converters) is approximately 96%.

This topology, as said before, is able to produce multilevel operation. Figure 26 shows the AC voltage waveforms and its 9 levels, measured without inductive filters.

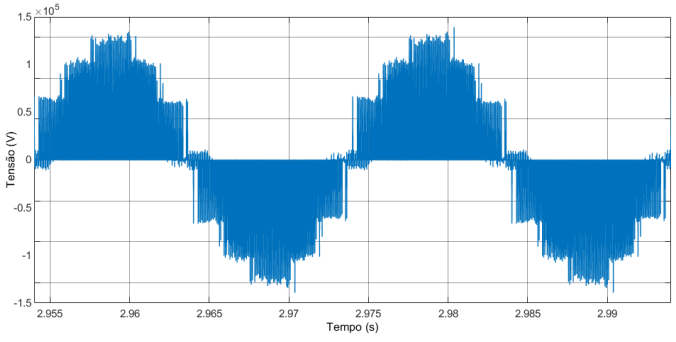

Figure 26: Nine-level AC voltage measured on transformer primary side without filters.

5.2. Transient Operation

In this analysis, the power reference was set to its nominal value and, after the system reached the permanent regime, the reference value was changed to 40% of the nominal power.

In Figure 27 are the measured power in a pair of converters and the power variation described.

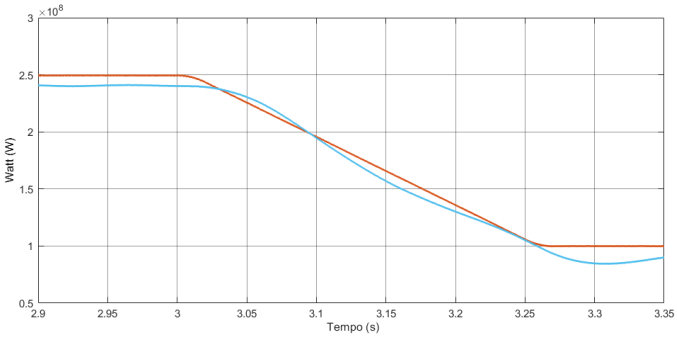

Figure 27: Half of the transmitted power - nominal power as reference and reduction to 40% of its value. Emitted power in orange and received power in blue.

In Figure 28 the variation in the amplitude of the three-phase currents can be observed, which results as a consequence of the power controller changing its reference, demonstrated in Figure 29. Furthermore, the voltage controller reference is also readjusted in order to maintain the same voltage level while the transmitted power value varies, as demonstrated in Figure 30.

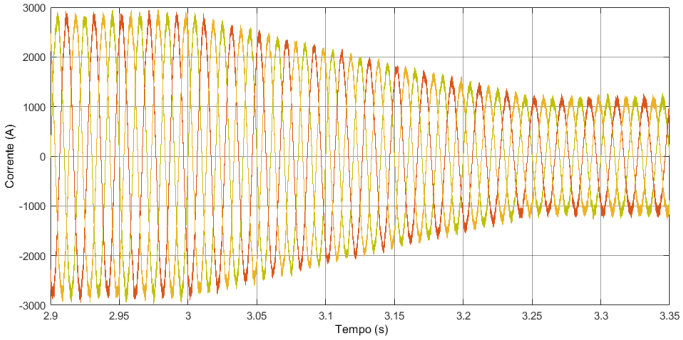

Figure 28: Transient three-phase currents on the receiver side.

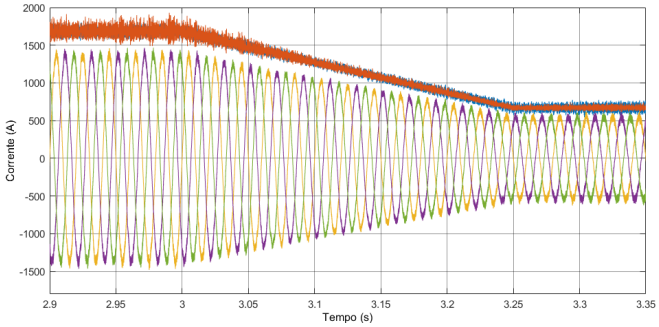

(a) Controlled currents to follow reference signal (in orange) after changing it.

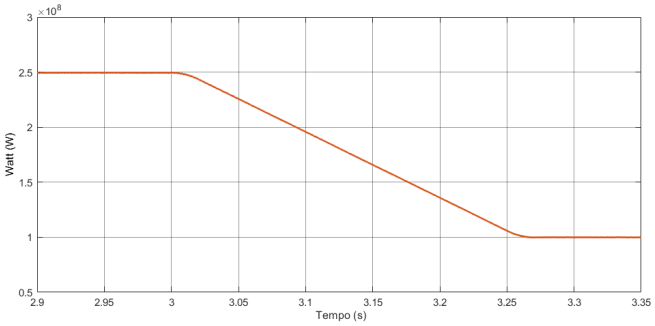

(b) Controlled power transient.

Figure 29: Power controller in transient operation.

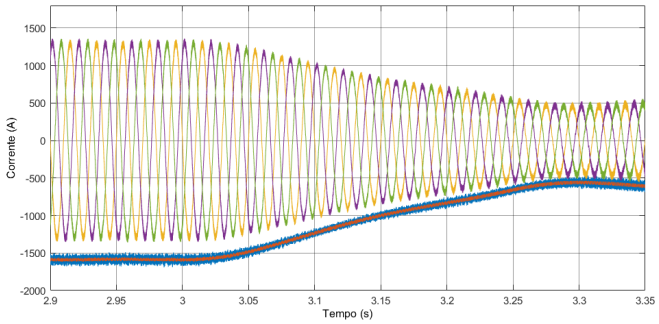

(a) Controlled currents following reference signal (in orange).

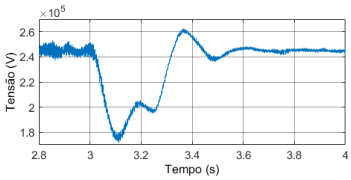

(b) Transient of the controlled voltage U_{dc} for a change in the reference power.

Figure 30: Voltage controller in transient operation.

In Figures 31 and 32 the DC transmission voltages and positive currents on the transmission lines as well as their transient behaviour are depicted.

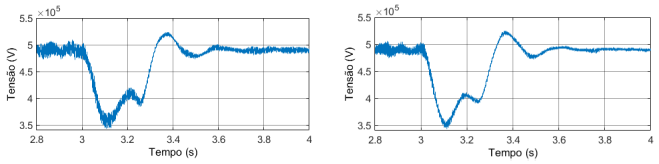

(a) Transmission voltage between converters 1 and 2.

(b) Transmission voltage between converters 3 and 4.

Figure 31: Transmission voltage between each pair of transmission lines.

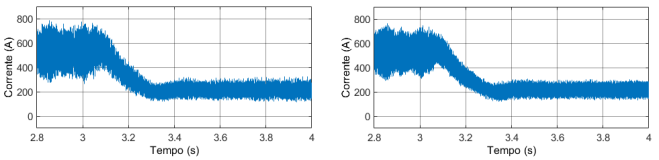

(a) DC current flowing through converters 1 and 2.

(b) DC current flowing through converters 3 and 4.

Figure 32: Transmission current flowing through positive transmission lines.

6. Conclusions and Future Work

6.1. Conclusions

A system was developed consisting of two transformers with open-end windings and four converters on each side of the system, with each pair of converters connected in series. This configuration of converters in series allows the transmission voltage to be doubled to twice the voltage for which the converters are dimensioned, while the parallel use of converters associated with the open-winding transformers allows multilevel operation.

Regarding the modelling of the system, for a correct and robust operation the necessary controllers were developed and the inductive and passive RLC series filters were designed. Furthermore, the π model was also used to represent the electrical transmission lines.

The most important conclusions to be drawn from the results obtained in this dissertation are the following:

- Multi-level operation can be achieved using two-level three-phase converters that can be linked in series in a new topology to obtain very high DC voltages;
- It is possible to control three-phase two-level converters in multilevel operation using the well-known sinusoidal pulse-width modulators;
- It was possible to design a controller architecture capable of controlling active powers injected into the DC line, reactive powers in the terminal AC networks, as well as the transmission voltages, using internal controllers of the AC currents of two converters in series;
- Overall efficiency is close to 96%, including losses in the DC lines;
- By designing suitable but simple filters it is possible to reduce the distortion of AC voltages and currents significantly. HV standards impose a maximum distortion of less than 5%, making the filter a key component of the topology;
- The ripple of DC currents and voltages indicates that DC filters are also required.

6.2. Future Work

In order to improve the transmission system, some actions can be taken. Other types of filters can be designed in order to further reduce the harmonic distortion.

Other types of controllers can be developed, as for example non-linear or space vector controllers in order to improve the accuracy of the system to reach the set reference values and to allow the system to reach the steady state state faster.

This topology can be extended to contain more converters in series by simply adding more converters connected in series to the existing pairs and more transformers (or more groups of three windings in the existing transformers), so it is possible to work with three-phase converters with fewer semiconductors in series, even for very high voltage. By de-phasing the AC voltages, and with a greater number of levels, which will allow harmonic distortion to be reduced and savings to be made on filters.

Finally, considering that this dissertation was based on the simulation of the developed topology, a physical prototype can be built at scale to test in laboratory.

References

[1] N. Flourentzou, V. G. Agelidis, and G. D. Demetriades. Vsc-based hvdc power transmission systems: An overview. *IEEE Transactions on power electronics*, 24(3):592–602, 2009.

[2] V. F. Pires, J. Fialho, and J. F. Silva. Hvdc transmission system using multilevel power converters based on dual three-phase two-level inverters. *International Journal of Electrical Power & Energy Systems*, 65:191–200, 2015.

[3] U. Corbellini and P. Pelacchi. Corona losses in hvdc bipolar lines. *IEEE Transactions on Power Delivery*, 11(3):1475–1481, 1996. doi: 10.1109/61.517506.

[4] C. K. Arruda and A. C. Lima. Corona modeling in hvdc transmission lines based on a modified particle-in-cell approach. *Electric Power Systems Research*, 125:91–99, 2015.

[5] J. P. Sucena Paiva. *Redes de Energia Elétrica: uma análise sistémica*. IST Press, 2011.

[6] J. F. A. da Silva. *Electrónica industrial: semicondutores e conversores de potência*. Fundação Calouste Gulbenkian, 2013.